

Electromagnetic and Thermal Model Parameters

Marius-Constantin O.S. Popescu, Nikos E. Mastorakis, Cornelia A. Bulucea, Liliana N. Perescu-Popescu

Abstract— The study of thermal model structural parameters is performed in this paper. Electromagnetic parameters are derived with recourse of electromagnetic similitude laws, and theoretical results are validated with data from transformer manufacturers. Different methodologies to estimate thermal parameters with data from standardised heat-run tests are compared.

Keywords— Electromagnetic similitude laws, Electromagnetic and thermal parameters, Oil-filled transformers.

I. INTRODUCTION

DU E to the widespread and easily use of computer calculations, numerical models are fundamental tools for a great number of subjects under study. Many parameters can intervene on transformer thermal model, depending upon models refinement. Electrical parameters such as load and no-load losses, can be directly determined from transformer data sheet and standardised tests. Thermal parameters such as the transformer thermal time constant and the oil temperature rise must be determined from specific tests and, usually, are not referred on data sheets. Electrical parameters are of much precise determination than thermal parameters. This work concerns the estimation of structural parameters of transformer thermal model, based upon electromagnetic similitude laws and real standardised transformer characteristics.

According to International Standards classification, a distribution transformer presents a maximum rating of 2500 kVA and a high-voltage rating limited to 33 kV; within such a large power range, design and project problems for the lower to the higher power transformers, are quite different. For studying a large power range of transformers, for which only the main characteristics are known, one can use the model theory; this method is largely established.

Marius-Constantin Popescu is currently an Associate Professor in Faculty of Electromechanical and Environmental Engineering, Electromechanical Engineering Department, University of Craiova, ROMANIA, e.mail address popescu.marius.c@gmail.com.

Nikos Mastorakis is currently a Professor in the Technical University of Sofia, BULGARIA, Professor at ASEI (Military Institutes of University Education), Hellenic Naval Academy, GREECE, e.mail address mastor@wseas.org.

Cornelia Aida Bulucea is currently an Associate Professor in Faculty of Electromechanical and Environmental Engineering, Electromechanical Engineering Department, University of Craiova, ROMANIA, e.mail address abulucea@gmail.com.

Liliana Perescu-Popescu is currently a Teacher in College Elena Cuza from Craiova, ROMANIA, e.mail address lpopi2001@yahoo.com.

"The most practicable way of determining the characteristics of apparatus embodying non-linear materials such as magnetic core ones, is usually experimental; analysis, while often valuable, is largely empirical and must therefore be verified by actual experimental data. By the use of model theory, however, the experimental data obtained on one unit, can be made to apply to all geometrically similar units, regardless of size, provided certain similarity conditions are observed" [13]. General similitude relationships for main characteristics of ONAN (*Oil Natural Air Natural*) cooled transformers within a power range from 25 kVA to 2500 kVA will be deduced on section 2. Transformer main characteristics that will be studied are: no-load magnetic losses, short-circuit Joule losses, transformer total mass, transformer oil mass. Similitude relationships will allow the definition of these characteristics as functions of transformer apparent rated power. Some of these characteristics are dependent upon the magnetic flux density, on the transformer magnetic circuit and current density, on the electrical circuit. In fact, since electrical and magnetic circuits are interlinked, any alteration in one of these circuits will lead to modifications on the other. Magnetic flux density and current density relationship will be analysed on section 3.

The accuracy of a given model is dependent upon the representative ness of the phenomenon one is interested on. The structure of the model can be more or less refined so that it will represent the phenomenon with a higher or lower degree of error. But its accuracy is also a function of the precision in estimating the parameters they are dependent upon; a highly elaborated model which parameters were careless determined would be of reduced interest. On section 4 theoretical similitude relationships are validated with information from data sheets, available at the moment of the study, relatively to realistic standardised transformers [1], [4], [25] and [24]. Numerical values resulting from data analysis are given in the form of confidence intervals, traducing their probabilistic character.

Other important aspect in the transformer parameters estimation is the time investment (and so, cost) involved in their determination; a compromise must be met between parameters precision and the corresponding procedure involved. This aspect is particularly relevant on the estimation of thermal parameters based on heat run tests. On section 5 a comparative study between methodologies to estimate transformer thermal time constant and final top-oil temperature rise is presented. The study is illustrated with a numerical example. Similitude relationships for these two parameters are also deduced.

II. SIMILITUDE RELATIONSHIPS FOR ELECTROMAGNETIC PARAMETERS

Similitude relationships will be established with the help of a generic transformer linear dimension, represented by l . It will be considered that this linear dimension, l_i , of an i transformer from the studied power range, will be related to the same linear dimension, l_j , of other j transformer of the same range, through an geometric relation of the form:

$$l_i = kl_j, \quad (1)$$

being k a constant (scale factor).

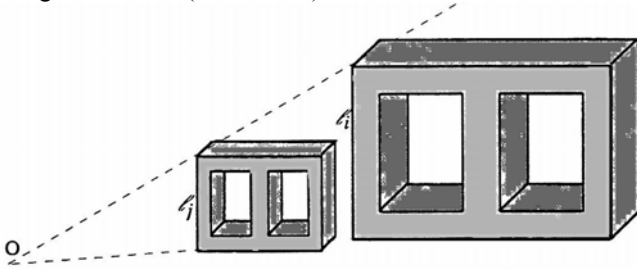


Fig. 1 - Geometric transformation (scale factor).

Transformer main characteristics that will be studied are: no-load magnetic losses, P_o , short-circuit Joule losses, P_{cc} , transformer total mass, M_T , transformer oil mass, M_o , main thermal time constant, τ_0 . Similitude relationships will allow the definition of these characteristics as functions of transformer rated power, S_R .

Unless particular conditions specified, general assumptions on next expression derivation are:

- i) frequencies involved in time varying characteristics are sufficiently low so that state can be considered quasi-stationary.
- ii) materials are magnetically, electrically and thermally homogeneous.
- iii) magnetic flux density is sinusoidal time-varying, always perpendicular to the core section and uniform at any cross section.

A. Rated power

Consider the elementary electromagnetic circuit of Figure 2, representing a winding of n_w turns, with an iron core where a sinusoidal varying magnetic flux density B is assumed. Conditions stated on section 2 are assumed.

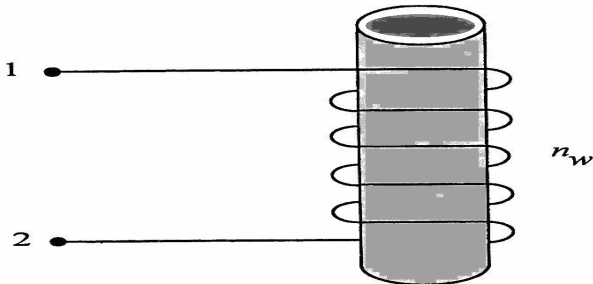


Fig. 2 - Elementary electromagnetic circuit representing a winding with n turns.

Neglecting the voltage drop due to winding resistance, the rated RMS value of the induced voltage per winding turn on terminals 1-2, U_e , is given by:

$$U_e = \frac{1}{\sqrt{2}} \omega B_{Max} A_c, \quad (2)$$

where: U_e induced voltage (RMS value) per winding turn [V], B_{Max} maximum magnetic flux density value on magnetic circuit [T], ω angular frequency [$\text{rad}\cdot\text{s}^{-1}$], A_c core cross-section [m^2].

Also, the rated RMS value of the winding current, I_R , can be defined as:

$$I_R = A_e J_R, \quad (3)$$

with: I_R rated current (RMS value) [A], J_R rated current density (RMS value) [$\text{A}\cdot\text{m}^{-2}$], A_e winding turn cross-section [m^2].

From (2) and (3), the rated power at terminals 1-2, denoted by S_R , will be given by:

$$S_R = \frac{1}{\sqrt{2}} \omega B_{Max} A_c n_w A_e J_R. \quad (4)$$

Using the linear dimension l , and considering that frequency, as well as the number of winding turns are invariant, expression (5) can be written as:

$$S_R \propto l^4 B_{Max} J_R. \quad (5)$$

Expression (5) means that, for a given pair of B_{Max} and J_R values, the rated power will increase proportionally to the fourth power of the transformer linear dimension.

B. Mass and volume

For the *Mass* and *Volume* study, the transformer will be considered as an homogeneous body with an equivalent volumic density, m_{veq} . Mass, is, therefore, traduced by:

$$M = m_{veq} V, \quad (6)$$

with: M transformer mass [kg], m_{veq} mas per unit volume [$\text{kg}\cdot\text{m}^{-3}$], V transformer volume [m^3] and thus, in terms of linear dimensions, both M and V will be proportional to the third power of transformer linear dimension

$$M, V \propto l^3. \quad (7)$$

C. Joule power losses without skin effect

In the absence of current harmonics, losses due to transformer variable load are essentially due to the flowing of the current through winding DC resistance, also referred as Joule losses, P_{winDC} . According to [10], these losses can be determined from a transformer short circuit test, under rated current. Due to their reduced value under this situation, one can neglect magnetic power losses on core and so, short-circuit power losses will be given, essentially, by Joule losses on windings. Under rated current it will be:

$$P_{cc} \approx P_{winDC} R = \frac{1}{\gamma_w} \frac{l_w}{A_e} I_R^2, \quad (8)$$

with:

γ_w electrical conductivity of windings material [$\Omega^{-1} \text{ m}^{-1}$],
 l_w windings wiring length [m].

On (8) derivation one is not taking into account losses due to skin effect. This effect arises in conductors carrying alternating currents and can be traduced by a non-uniform current density caused by the varying magnetic field produced within the conductor by its own current, as well as by its neighbouring conductors. When the load current of a transformer increases, this usually give rise to an increase of eddy and hysteresis losses, even without a change in the core magnetic flux, due to this skin effect - these losses are called *stray load losses*.

Stray load losses increase with the frequency of the current and with the size of the conductors. To reduce these losses, similarly to the core lamination, also, in properly designed transformers, large section conductors are subdivided into several conductors of small section, insulated from each other and suitable transposed throughout the windings, so that skin effect is minimised. For the purpose of this similarity study, stray losses will be neglected.

Attending to (3) expression (8) can be rewritten as:

$$P_{cc} \approx \frac{1}{\gamma_w} \frac{l_w}{A_e} (A_e J_R)^2. \quad (9)$$

For this similitude study, a constant ambient temperature scenario can be assumed, and so the resistivity of the windings material can be considered a constant value, resulting, for the short-circuit power losses, the expression:

$$P_{cc} \propto J_R^2 l^3. \quad (10)$$

Expression (10) means that, for a given value of current density, load losses will increase with the third power of the core linear dimensions.

D. No-load power losses

Under transformer no-load situation, the losses that occur in the material arise from two causes:

i) the tendency of the material to retain magnetism or to oppose a change in magnetism, often referred to as magnetic hysteresis

ii) the RI^2 heating which appears in the material as a result of the voltages and consequent circulatory currents induced in it by the time variation of the flux.

The first of these contributions to the energy dissipation is known as *hysteresis power losses*, P_H , and the second, as *eddy current power losses*, P_E , at a constant industrial frequency. Attending to the general approach of this study and to their reduced value under no-load operation, Joule power losses due to magnetisation current will be neglected, as well as any other additional power losses. According to [2], eddy current power losses can be traduced by:

$$P_E = \frac{\omega^2 \gamma_c}{24} \varepsilon^2 B_{Max}^2 V_{core}, \quad (11)$$

with: γ_c electrical conductivity of magnetic sheets (Fe-Si) per unit volume [$\Omega^{-1} \text{ m}^{-3}$], ε thickness of magnetic sheets [m], V_{core} effective core volume [m^3].

The thickness of the core sheets will be consider constant, within the analysed power range, and therefore:

$$P_E \propto B_{Max}^2 l^3. \quad (12)$$

For the hysteresis losses on a magnetic circuit of volume V in which the magnetic flux density is everywhere uniform and varying cyclically at a frequency ω , the empirical Steinmetz expression [2], will be considered:

$$P_H = \frac{\omega}{2\pi} k_H V B_{Max}^\nu, \quad (13)$$

with: k_H hysteresis coefficient (material characteristics), ν empirical Steinmetz exponent (it can vary from 1,6 to 2,5).

For the usual Fe-Si sheets, one can consider that $\nu=2$ and thus (13) can be rewritten as:

$$P_H \propto B_{Max}^2 l^3. \quad (14)$$

Attending to (12), the proportionality relationship for no-load power losses will be given by:

$$P_0 \propto B_{Max}^2 l^3. \quad (15)$$

Expression (15) traduces the proportionality of no-load power losses with the third power of transformer linear dimension (volume) for each given value of magnetic flux density. Table 1 regroups the basic similitude relationships deduced on previous paragraphs and which will be developed on next sections.

Table 1. Basic similitude relationships.

| | | | |
|-------------------------------|--------------------------|-----------------------------|--------------------|
| $J_R \propto l^4 B_{Max} J_R$ | $P_{CC} \propto l^3 J_R$ | $P_0 \propto l^3 B_{Max}^2$ | $M, V \propto l^3$ |
|-------------------------------|--------------------------|-----------------------------|--------------------|

Apart from *Mass* and *Volume* all these transformer characteristics depend upon B_{Max} and J_R evolutions within the considered power range; these evolutions will be analysed on next section.

III. THE RELATIONSHIP BETWEEN B AND J

Magnetic and electrical circuits are interlinked; in particular, the magnetic field H in the transformer core is interlinked with the magnetisation density current, J_μ , through the Ampere law:

$$\oint H ds = \iint (J_\mu \bar{n}) dA. \quad (16)$$

The non-linear nature and complexity of the magnetisation phenomena are traduced by:

$$B = \mu(H)H . \quad (17)$$

However, in a simplified way, attending to the generalisation of this study and according to general assumptions defined on §2 one can approximate (17) to:

$$R_m A_c B = n_w J_\mu A_e , \quad (18)$$

with: R_m magnetic circuit reluctance [H^{-1}].

Introducing the linear dimension l in expression (18) one obtains:

$$B \propto J_\mu l . \quad (19)$$

From expression (19) one can conclude that, B and J_μ values could not be maintained constants after a change in the transformers size.

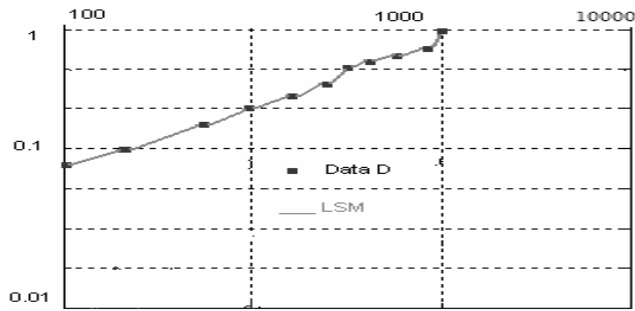


Fig. 3 - Magnetisation current (in p.u. values of rated current) as a function of transformer rated power.

Expression (19) can not be directly validated since B values are not usually available on transformers data sheet. Only magnetisation current data values were available from one of the considered transformer manufacturers [25], [19]. Magnetisation current data values are represented on Figure 3, as per unit values of transformer rated current and as a function of the transformer rated power.

One should recall that expression (19) is valid only for the non-saturation zone of magnetisation curve and it concerns only to the magnetisation density current, J_μ , not windings rated density current, J_R .

For technical and economical reasons B value is not fixed on the non-saturation zone of the magnetisation curve, but on the intermediate zone between the non-saturation and the saturation zones.

From an economical point of view, it is most desirable to have high B values, in order to allow the reduction of core cross-section for a same value of flux. With this procedure, iron volume reduction can be achieved.

On the other hand, from the technical point of view, high B values would lead to magnetic saturation phenomena and therefore, to highly distorted transient magnetisation currents with important amplitude values (international standards limit these transient currents in per cent values of rated current).

Moreover, high B values increase hysteresis losses (by increasing the hysteresis area) and thus, decreasing the transformer efficiency.

This dual compromise between technical and economical aspects leads to the rated B value to be fixed near the knee of the magnetisation curve, B_{Max} . This value depends upon the used material, the manufacturing technology, etc; most common values are between 1.75 and 1.85 T [2], allowing as well, the magnetisation current to be limited within standard limits. Therefore, for this similitude study purpose, it will be considered that:

$$B = B_{Max} = ct. \quad (20)$$

Attending to Table 1 basic similitude relationships for P_{cc} and P_o , one realises that current density J_R , performs in P_{cc} expression, an analogous role as B_{Max} performs in P_o one. The relationship between J_R and B_{Max} could then be studied through the relationship between P_{cc} and P_o .

Figure 4 represents a scatter diagram of P_{cc} and P_o values from several distribution transformers of four different manufacturers. Generally, a relationship between P_{cc} and P_o values of the form:

$$P_{cc} \propto P_o^\beta , \quad (21)$$

can be assumed and in the next two sections two hypotheses will be analysed, namely:

- i) There is no linear relationship between P_{cc} and P_o values (and therefore, $\beta \neq 1$),
- ii) There is a linear relationship between P_{cc} and P_o values (and therefore, $\beta = 1$).

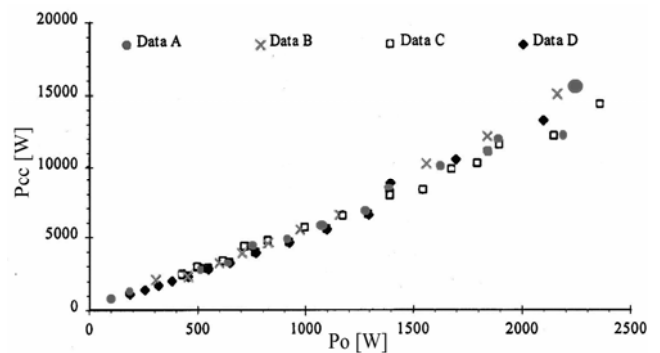


Fig. 4 - Scatter Diagram of short-circuit and no-load power losses.

A. Constant B value

Considering the general case of expression (21), attending to (10), and B_{Max} as invariant, one concludes that current density J_R must be:

$$J_R \propto l^{\frac{3(\beta-1)}{2}} . \quad (22)$$

Using expression (22) on Table 2, one gets:

Table 2. Basic expressions for similitude laws considering $B = \text{constant}$.

| | | | |
|--------------------------------|-----------------------------|-------------------|--------------------|
| $S_R \propto l^{(5+3\beta)/2}$ | $P_{CC} \propto l^{3\beta}$ | $P_o \propto l^3$ | $M, V \propto l^3$ |
|--------------------------------|-----------------------------|-------------------|--------------------|

Table 3. Similitude relationships considering $B = ct$.

| | | |
|--|----------------------------------|-----------------------------------|
| $P_{CC} \propto S_R^{6\beta/(5+3\beta)}$ | $P_0 \propto S_R^{6/(5+3\beta)}$ | $M, V \propto S_R^{6/(5+3\beta)}$ |
|--|----------------------------------|-----------------------------------|

Expressions of Table 2 and Table 3 represent the general case for P_{cc} , P_o and M, V evolution with S_R , assuming the relationship of expression (21); for $\beta = 1$, expressions will represent the particularly case of a linear relationship between P_{cc} and P_o values.

B. Constants B and J values

Assuming the transformer will operate under a constant given load-factor, one of the most common design trade-offs to maximise its efficiency, is achieved by choosing the most convenient P_o/P_{cc} ratio. This is traduced by the manufacturers well-known relationship:

$$K_{\eta_{max}} = \sqrt{P_0 / P_{cc}}, \quad (23)$$

with: $K_{\eta_{max}}$ maximum efficiency load-factor [p.u].

Figure 5 represents this maximum efficiency load factor, for the considered transformer power range. From Figure 5 it is reasonable to consider that this maximum efficiency load-factor is approximately the same for all transformers of the analysed power range; from this assumption one derives the following relation:

$$P_{cc} \propto P_0. \quad (24)$$

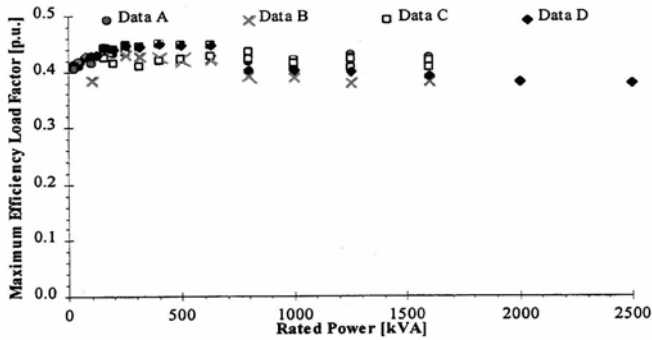


Fig. 5 - Maximum efficiency load factor as a function of rated power.

From expression (24) and attending to P_o and P_{cc} similitude relationships, expressions (10) and (15), one concludes that:

$$J_R \propto B_{Max} \quad (25)$$

and thus, being B_{Max} value fixed, so will be J_R ,

$$J_R = ct. \quad (26)$$

and J_R fixed values, expressions of Table 1 become:

Table 4. Similitude relationships for $B = ct$ and $J = ct$.

| | | | |
|-------------------|----------------------|-------------------|--------------------|
| $S_R \propto l^4$ | $P_{CC} \propto l^3$ | $P_0 \propto l^3$ | $M, V \propto l^3$ |
|-------------------|----------------------|-------------------|--------------------|

In terms of S_R , expressions of Table 4 become:

Table 5. Similitude relationships for $B = ct$ and $J = ct$.

| | | |
|------------------------------|---------------------------|----------------------------|
| $P_{CC} \propto S_R^{0.750}$ | $P_0 \propto S_R^{0.750}$ | $M, V \propto S_R^{0.750}$ |
|------------------------------|---------------------------|----------------------------|

As mentioned before, these expressions are Table 2 and Table 3 ones with $\beta = 1$. The graphical representation and analysis of expressions from Table 3 and Table 5, as well as their validation with data values from different distribution transformer manufacturers will be performed on section 4.

IV. EXPRESSIONS VALIDATION

The validation of theoretical similitude relationships established on Table 3 and Table 5, will be performed, with data from four different distribution transformers manufacturers (referred as "A", "B", "C" and "D"). Transformer rated voltage ranges from 6 to 36 kV and rated power from 25 to 2500 kVA. All transformers are oil-immersed and ONAN refrigerated [15].

The numerical fitting method used was the *Least Square Method* in its Simple (LSM) and *Weighted* versions (WLSM) [7]. Fitting expressions are of the form:

$$x = s^c, \quad (27)$$

where x represent generic characteristics m, p_{cc}, p_o, v and τ_{pu} [p.u.], which are p.u. variables defined according to:

$$\begin{aligned} s &\equiv S_R / S_{R0} ; & p_{cc} &\equiv P_{cc} / P_{cc0} ; & P_0 &\equiv P_0 / P_{00} \\ m &\equiv M / M_0 ; & v &\equiv V / V_0 ; & \tau_{pu} &\equiv \tau_0 / \tau_{00} \end{aligned}$$

being the p.u. base given by characteristics of a 160 kVA reference transformer:

$$\begin{aligned} S_{R0} &= 160 \text{ kVA} ; & P_{cc0} &= 2350 \text{ W} ; & P_{00} &= 460 \text{ W} \\ M_0 &= 720 \text{ kg} ; & V_0 &= 0,959 \text{ m}^3 ; & \tau_{00} &= 2 \text{ h} \end{aligned}$$

A. Short-circuit and no-load power losses relationship

As mentioned on section 3, the assumed relationship between P_{cc} and P_o is of the form:

$$P_{CC} \propto P_0^\beta. \quad (28)$$

Considering it a linear relationship ($\beta = 1$), previous expression leads to the conclusion that both B_{Max} and J_R must be constant values, and thus expressions from Table 2 and Table 3 should be used. If the relationship is not linear ($\beta \neq 1$), B_{Max} will still be a constant value but J_R must increase according to (22), resulting in expressions represented on Table 4 and Table 5.

From the *Least Square Method* (LSM) and with data represented in Figure 4, one can obtain the maximum likelihood estimator of β , denoted by $\hat{\beta}$. This estimator being a random variable normally distributed [3], [18] presents the

following first moments (mean and standard deviation) values, denoted by $\mu_{\hat{\beta}}$ and $\sigma_{\hat{\beta}}$, respectively:

$$\mu_{\hat{\beta}} = 1.021 \quad \text{and} \quad \sigma_{\hat{\beta}} = 0.013. \quad (29)$$

The 95% confidence interval of estimator $\hat{\beta}$ is delimited by [0.996; 1.046]. This statistical analysis, by including the value $\beta=1$ on the 95% confidence interval, does not exclude the hypotheses of a linear relationship between P_{cc} and P_o values. From the statistical analysis no conclusion can be drawn about whether or not the relationship between P_{cc} and P_o is linear but the hypotheses of a linear relationship is not excluded. Due to the closeness of obtained $\mu_{\hat{\beta}}$ value with unit and since this

divergence can be justified by approximations on P_{cc} and P_o data values, it will be considered that P_{cc} and P_o are related by a linear relationship. Therefore, the set of expressions to validate is that represented on Table 5. Data, regression function as well as the 95% confidence limits are represented, in logarithmic scales, on Figure 6.

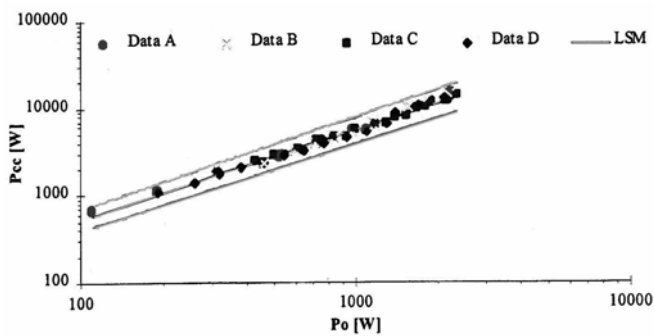


Fig. 6 - Short-circuit and No-load power losses; regression line and 95% confidence limits.

B. Mass and volume

On Figure 7 is represented, in logarithmic scale, data from the catalogue and the regression lines obtained with the LSM, representing the theoretical expression of M (or V), as a function of rated power. On Figure 7, is clear that the mass of lower rated power transformers deflects from the regression line and approaches it bests, as rated power increases.

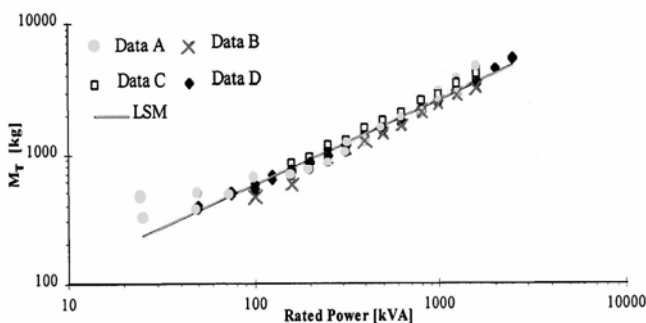


Fig. 7 - Transformer total mass; regression line. Theoretical Expression $m, v = s^{0.750}$.

The non-considered aspects of the theoretical model can explain this scale phenomenon. When modelling *Mass*, one

should take into account that, when considering the transformer as a whole, there are "fixed weights", like bushings, tap-changer, conservator and accessories in general, that will not increase with the theoretical 0.750 power of rated power. The developed theoretical model does not take into account these "fixed weights". To strengthen this justification, and as will be clear when analysing the characteristic "No-load Losses", this scale phenomenon is not present on core mass, which is an important portion of the transformer total weight; core mass evolution with rated power is quite near theoretical behaviour. Substituting ζ by the mean value of its estimator, $\hat{\zeta}$, obtained with the LSM fitting method, the resulting regression expression is:

$$m, v = s^{0.656}, \quad (30)$$

with a standard deviation $\sigma_{\hat{\zeta}}=0.012$ and a 95% confidence interval delimited by [0.633; 0.677].

The relative lower value of $\hat{\zeta}$ (0.656), relatively to the theoretical 0.750 value, is explained by the scale phenomena above mentioned. Due to this scale phenomenon and considering that large rated power transformers fit theoretical model best, the *Weight Least Square Method* (WLSM) fitting method was employed. Normalised weight (w_i) should decrease with rated power according to:

$$w_i = 1/S_{R_i}, \quad (31)$$

being S_{R_i} a normalised value of the transformer i rated power.

The assumed base value for normalisation was the maximum value of rated powers within the considered power range. In this manner, WLSM approach will put the greatest emphasis on higher rated power transformers, according to the assumption that higher rated power transformers will fit theoretical model best. Substituting ζ by the mean value of its estimator, $\hat{\zeta}$, obtained with the WLSM fitting method, the resulting regression expression is:

$$m, v = s^{0.711}, \quad (32)$$

with a standard deviation $\sigma_{\hat{\zeta}}=0.012$ and a 95% confidence interval delimited by [0.692; 0.737]. Fitted line resulting from WLSM as well as 95% confidence limits are represented on Figure 8. As expected, $\hat{\zeta}$ value approached the theoretical value. If the analysis is performed only considering transformers with rate power above 200 kVA, $\hat{\zeta}$ mean value with the LSM method increases to 0.730, with $\sigma_{\hat{\zeta}}=0.014$ and the 95% confidence interval is shifted to [0.702; 0.758], which, including the theoretical value 0.750, validates the theoretical model.

C. Oil mass

Since the oil mass represents an important role in thermal characteristics of transformers and its mass is about 17 to 25% of the transformer total mass, the same kind of analysis performed for *Total Mass* will be developed for transformers

oil mass. Results graphical representation is on Figure 9. Manufacturer C data was not available on catalogue data.

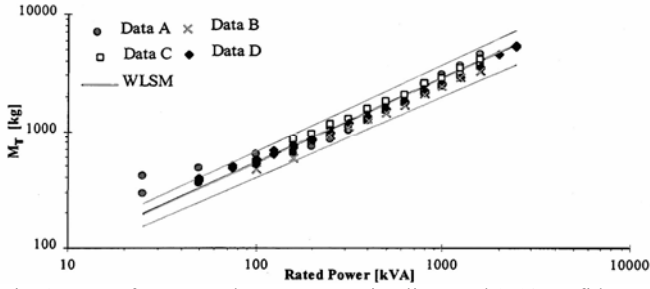


Fig. 8 - Transformer total mass; regression lines and 95% confidence limits for WLSM.

Data dispersion is greater than verified on transformers total mass, and the scale phenomena, although not so strongly, is still present. On Figure 9 transformers rated voltage within each manufacturer are referred, in order to evidence that each series verifies theoretical model much better than global data.

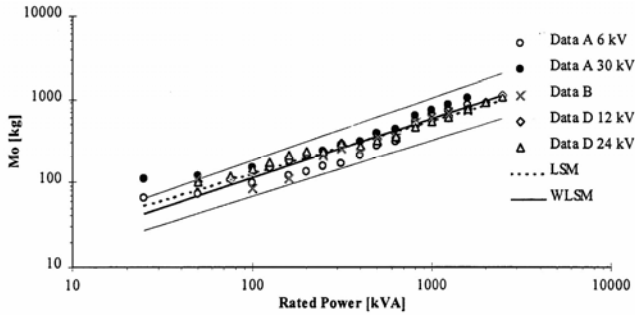


Fig. 9 - Transformer oil mass; regression lines and 95% confidence interval for WLSM. Theoretical Expression $m, v = s^{0.750}$.

Estimator values obtained with LSM and WLSM fitting methods lead to the following two set of expressions:

$$m, v = s^{0.286}, \quad (33)$$

for LSM, with $\sigma_{\hat{\zeta}} = 0.022$ and 95% confidence interval delimited by [0.585; 0.671], and

$$m, v = s^{0.711}, \quad (34)$$

for the WLSM method, with $\sigma_{\hat{\zeta}} = 0.022$ and 95% confidence interval delimited by [0.668; 0.754]. On Figure 9, line resulting from LSM method is represented with as dotted and the one resulting from WLSM, as well as its 95% confidence limits, with straight lines. The improvement in the ξ value, achieved with the WLSM method, validates the theoretical expression.

D. Short-circuit power losses

Figure 10 represents P_{cc} relationship with rated power.

The expression resulting from mean values of estimator obtained with the LSM fitting, is:

$$P_{cc} = s^{0.784}, \quad (35)$$

with $\sigma_{\hat{\zeta}} = 0.009$ and the 95% confidence interval limited by [0.766; 0.802].

As clear on graphical representation, there is no scale phenomenon and results fit theoretical expectations very well.

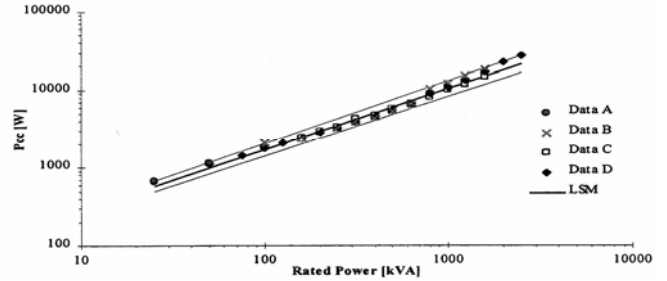


Fig. 10 - Short-circuit power losses, as a function of rated power; regression line and 95% confidence limits. Theoretical Expression $P_{cc} = s^{0.750}$.

E. No-load power losses

Figure 11 represents no-load power loss evolution with rated power. Like short-circuit power losses, no-load power loss show no scale phenomena around lower rated power transformers. Resulting expression from estimator obtained with the LSM fitting method is:

$$P_0 = s^{0.748}, \quad (36)$$

with $\sigma_{\hat{\zeta}} = 0.005$ and the 95% confidence interval delimited by [0.739; 0.757].

No-load power loss values fit very well the theoretical relationship. Moreover, being no-load power losses related to core mass (assuming that core material is the same within the consider power range), one can infer that core mass, also, fits very well the theoretical relationship:

$$CoreMass = s^{0.750}, \quad (37)$$

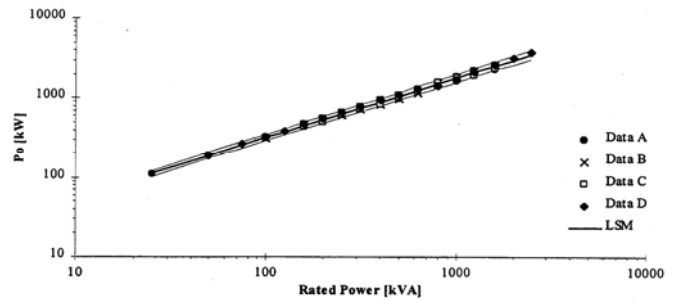


Fig. 11 - No-load power losses, as a function of rated power, regression line and 95% confidence limits.

This conclusion lets clear that the scale phenomena verified when analysing the transformer total mass is due, mainly, to the mass of transformers "fixed weights", such as bushings, tap-changer, conservator and accessories in general.

V. THERMAL PARAMETERS

The linear first order thermal model presented in International Standards and derived on [16], is considered a

reference; to use it, knowledge of transformer main thermal time constant, τ_0 , as well as final top-oil temperature rise under rated load, $\Delta\Theta_o$, is needed. Usually, these two parameters are determined using data from a heat-run test, although estimation with data from the cooling curve is also possible [12], as well as on-line estimation from a monitoring system [14].

Several methodologies can be found to estimate these two parameters from test data [5], [6], [11], [12], and [16]. Experimental constrains for their application are different for each methodology (the required time duration for the test, the necessity of equidistant measured values), graphical and numerical methodologies lead to different results and, some of them, do not allow estimation of parameters uncertainty.

On section §5.A, similitude relationships for τ_0 and $\Delta\Theta_o$ will be deduced. On section §5.B a comparative study between several methodologies used to estimate these two thermal parameters from heat run tests will be performed.

A. Similitude relationships

In agreement with the thermal model of the homogeneous body, the final temperature rise, $\Delta\Theta_f$, is dependent upon the total power losses generated inside the body, P_{loss} , the external cooling surface, A_s , and also upon the heat transfer coefficient, h_{cr} , as derived on:

$$\Delta\Theta_f = \frac{P_{loss}}{h_{cr}A_s}. \quad (38)$$

All losses in electrical power apparatus are converted into heat and insulation materials are the ones that suffer most from overheating; on windings insulation materials, overheat will slowly degrading materials thermal and chemical insulation properties and on oil, overheat will produce chemical decomposition, degrading its dielectric strength [9].

Since heating, rather than electrical or mechanical considerations directly, determines the permissible output of an apparatus, design project includes heating optimisation. Which means that each transformer will be designed to heat just the maximum admissible value, under normal rated conditions. The maximum safe continued load is the one at which the steady temperature is at the highest safe operating point. Reference [12] considers an hot-spot temperature of 98°C, for an ambient temperature of 20°C.

On a transformer, all the power losses are due to summation of constant voltage magnetic losses and variable current winding losses. Let total losses, under rated load, denoted by P_{lossR} , be approximated by:

$$P_{lossR} = P_{CC} + P_0. \quad (39)$$

Considering (38) and (39) and attending to similitude expressions for load and no-load losses, expressions (10) and (15), top-oil final temperature rise under rated load, $\Delta\Theta_{ofR}$, will be:

$$\Delta\Theta_{ofR} \propto \left(J_R^2 + B_{Max}^2 \right). \quad (40)$$

Considering B_{Max} and J_R are constant values, final transformer temperature rise would increase with the first power of linear dimension:

$$\Delta\Theta_{ofR} \propto l. \quad (41)$$

If only B_{Max} is a constant value and J_R values increase according to (22), final temperature rise will still increase with transformer size. Therefore, regardless which hypothesis is consider, the final transformer temperature rise, will always be:

$$\Delta\Theta_{ofR} \propto l^\phi, \quad (42)$$

with an ϕ value equal or greater than the unity.

One could then conclude that final temperature rise of transformers would always rise with its linear dimension. In practice this fact does not occur because transformers refrigeration system is improved as rated power increases, by increasing the external cooling surface through corrugation. The effect of refrigeration improvement can be traduced by an equivalent refrigeration rate, $(h_{cr}A_s)_{eq}$, which increases with the third power of the linear dimension l .

$$(h_{cr}A_s)_{eq} \propto l^3. \quad (43)$$

Under these conditions, equation (41) can be rewritten as:

$$\Delta\Theta_f = \frac{P_{lossR}}{(h_{cr}A_s)_{eq}} = ct. \quad (44)$$

This expression, however, can not be validated with data since neither $\Delta\Theta_{ofR}$ nor $(h_{cr}A_s)_{eq}$ values are available on transformer data sheets. According to the thermal model of an homogeneous body, the thermal time constant, τ_0 , can be given by:

$$\tau = c_m M \frac{\Delta\Theta_f}{P_{loss}}. \quad (45)$$

On the lack of transformer thermal capacity knowledge, c_m , one of the approximate methods suggested by IEC 76-2 to estimate the transformer main thermal time constant, is based upon information available on transformer rating plate, this expression is reproduced on:

$$\tau_0 = \frac{5M_T + 15M_o}{P_{loss}} \Delta\Theta_{of}, \quad (46)$$

where M_T and M_o represent the transformer total and the oil masses, respectively.

Expression (46) derives from the assumption that, within an homogeneous transformer series, there is a constant proportion between transformer total mass and oil mass; coefficients affecting M_T and M_o reflect this assumed proportionality as well as different thermal capacities for each part. A similar relationship is suggested by [26]. Remark should be made that this is an approximate formula, and

therefore, resulting values will carry inherent errors. As an illustrative example is presented, relatively to an ONAN 160 kVA distribution transformer, 20/0.4 kV rated voltage, whose main time constant was estimated from two different methods. Since available data included transformer characteristics, oil mass, total mass and also the heating test from the manufacturer, main thermal time constant was estimated through heating test data, according to [11] proposed procedures. Extrapolation of all the points from the heating curve, led to a thermal time constant value of 1.9 hour; extrapolating only the upper 60% part of the heating curve, a more accurate value would be obtained [11] and that was 1.8 hour. On the other hand, using expression (46) the resulting value was 1.5 hour, which traduces the approximately character of this expression.

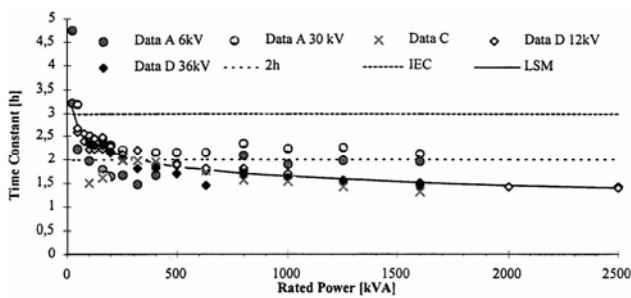


Fig. 12 - Thermal time constants, based on expression (46).

Usually, distribution transformers catalogues do not include thermal time constant values; nevertheless, they are of primordial importance in loss of life expectancy studies. In order to validate similitude expressions, values obtained through expression (46) will be used.

Since available data includes M_T , M_o and P_{loss} rated values, the thermal time constant, under rated losses, τ_0 , was determined, assuming that final top-oil temperature rise, $\Delta\Theta_{of}$, was 60 K for all transformers. This temperature rise is the maximal admissible value for top-oil temperature rise of oil-immersed transformers referred to steady state under continuous rated power [12]. With this assumption, the resulting τ_0 values will correspond to an overestimation and, therefore, transient hot spot temperatures will be underestimated, as well as consequent loss of life. Results are represented on Figure 12.

To describe the evolution of transformer thermal time constant with rated power, the following generic expression was assumed:

$$\tau_{pu} = s^\zeta. \quad (47)$$

With the LSM fitting method, the obtained mean value of the ζ estimator leads to:

$$\tau_{pu} = s^{-0.143}, \quad (48)$$

with $\sigma_\zeta = 0.016$ and the 95% confidence interval limited by [-0.174; -0.111].

Reference [12] proposes 3 hours for the thermal time constant value to be used on loss of life calculations, provided no other

value is given from the manufacturer. Attending to (46) and to the fact that the maximum admissible $\Delta\Theta_{of}$ value was assumed, the proposed value of 3 hours is of difficult justification. International guides are often referred as conservative ones; however, for loss of life considerations, a conservative value for transformer thermal time constant should not be a maximum value but, on the opposite, a minimum one. According to this study, which is based on expression (46), if a fixed value had to be assumed for the thermal time constant of distribution transformers, this value would be approximately 2 hours.

From expression (45), considering approximation (39), and introducing similitude expressions for M_T , P_o and P_{cc} presented in Table 4, the resulting similitude expression for transformer thermal time constant, under rated conditions, is:

$$\tau_0 \propto \frac{l^3}{l^{3\beta} + l^3}, \quad (49)$$

or, in terms of rated power (expressions from Table 5):

$$\tau_0 \propto \frac{S_R^{6/(5+3\beta)}}{S_R^{6/(5+3\beta)} + S_R^{6/(5+3\beta)}}. \quad (50)$$

Considering B_{Max} and J_R constant values for the transformer homogeneous series ($\beta=1$), expression (49) becomes:

$$\tau_0 \propto ct. \quad (51)$$

This result agrees with International Standards since they propose a fixed value of 3 hours for the thermal time constant of all distribution transformers [12]. Considering J_R evolution presented by (22) and using (3 mean value expressed on (29a), ($\mu_\beta=1.021$, thermal time constant evolution with rated power would be represented by:

$$\tau_0 \propto \frac{S_R^{0.744}}{S_R^{0.760} + S_R^{0.744}}. \quad (52)$$

This expression is represented on Figure 13. The scatter diagrams of Figure 12 and Figure 13 evidence a considerable dispersion of values for thermal time constant. Recalling that these thermal time constant values were not obtained from catalogue data, but through expression (46), this variance can be explained either by the approximate character of the expression, either by the high variance values of total and oil masses, already verified when analysing these transformer characteristics.

Regardless the hypotheses of J_R variation, constant or slightly increasing with transformer rated power, the conclusion regarding thermal time constant is similar: from similitude relationships the thermal time constant of distribution transformers are close to 2 hour.

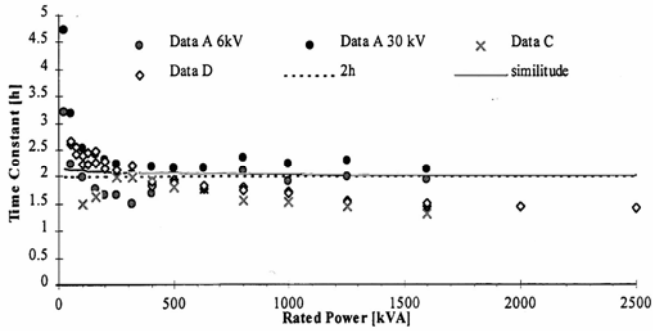


Fig. 13 - Thermal time constant and theoretical expression (52).

B. Thermal parameters estimation from tests

In this section transformer thermal time constant and final top-oil temperature rise under rated load, will be estimated. International Standards methodologies and methodology proposed in [16], will be applied to a single set of values from a simulated heat run test, so that "correct" parameter values are known in advance and results from different methodology can be compared [21].

B.1. International Standards Methodology

Existing methodologies can be classified into numerical and graphical ones. Both assume that the temperature rise, relatively to ambient temperature, of such a process can be approximated to a first order exponential process and therefore described by an increasing time exponential function:

$$\Delta\Theta_0(t) = \Delta\Theta_{of} \left(1 - e^{-t/\tau_0}\right), \quad (53)$$

where $\Delta\Theta_{of}$ denotes the final steady-state temperature rise of top-oil [K].

Method known as "three points method", [11], (TPM) derives directly from application of (53) to three equidistant data values $(t_1, \Delta\Theta_{o1})$, $(t_2, \Delta\Theta_{o2})$ and $(t_3, \Delta\Theta_{o3})$ such that $t_3 = t_2 + \Delta t = t_1 + 2 \Delta t$. It results:

$$\Delta\Theta_{of} = \frac{\Delta\Theta_{o2}^2 - \Delta\Theta_{o1}\Delta\Theta_{o3}}{2\Delta\Theta_{o2} - \Delta\Theta_{o1} - \Delta\Theta_{o3}} \quad \text{and} \quad (54)$$

$$\tau_0 = \frac{\Delta t}{\ln \frac{\Delta\Theta_{o2} - \Delta\Theta_{o1}}{\Delta\Theta_{o3} - \Delta\Theta_{o2}}}$$

Other method recommended by [11] is the "least square method" (LSM) based upon the minimisation of square errors between data values and theoretical heating function (53).

In practice, due to the complexity and non-linearity of thermal exchange, the transformer heating process is governed by more than one thermal time constant, [11], [12], possibly time or temperature dependent. Therefore, more accurate values are obtained by applying methodologies to the final part of the heating curve, when the effect of smaller thermal time constants (windings) is negligible, prevailing the effect of larger one, τ_0 . For this reason, and according to [11], successive estimates by the TPM should converge and, to avoid large random numerical errors, time interval Δt should

be of the same magnitude as τ_0 and $\Delta\Theta_{o3}/\Delta\Theta_{of}$ should not be less than 0.95, which, assuming (53) model, is equivalent to:

$$t_3 \geq 3\tau_0. \quad (55)$$

Similarly, the LSM should be applied only for the 60% upper part of the heating curve. Constrains for the TPM application are the necessity of equidistant measured data values and the time duration of the test given by (55).

Criterion to terminate the heat run test is [11]: *to maintain the test 3 more hours after the rate of change in temperature rise has fallen below 1K per hour, and take the average of last hour measures as the result of the test.* For long term tests, such as the required by [11], invariant process conditions are of difficult sustenance namely: the constancy in transformer losses (voltage, current, $\cos\phi$) and thermal exchange (ambient temperature, wind, sun).

B2. Alternative Method

Reference [16] proposes a new method to estimate $\Delta\Theta_{of}$ and τ_0 . Since (53) linearization, by a simple mathematical transformation, is not possible for unknown $\Delta\Theta_{of}$ and τ_0 parameters and truncated data, an approximation of (53) by a polynomial function is proposed:

$$1 - e^{-t/\tau_0} \approx \left(\frac{t}{\tau_0}\right) / \left[1 + \left(\frac{t}{\tau_0}\right)/6\right]^3. \quad (56)$$

The exponential function is a majoring of the polynomial function being the systematic error, ε_S , one commits with this approximation a function of the ratio t/τ_0 . This systematic error can be measured through:

$$\varepsilon_S = \frac{1 - e^{-t/\tau_0}}{(t/\tau_0) / [1 + (t/\tau_0)/6]^3} - 1. \quad (57)$$

A majoring of this systematic error, ε_M is:

$$\varepsilon_M = (t/\tau_0)^3 / 216. \quad (58)$$

Inserting approximation (57) into (53), one obtains:

$$f(\Delta\Theta(t), t) = a + bt, \quad (59)$$

being f a generic non-linear function and:

$$a = \left[\frac{\tau_0}{\Delta\Theta_{of}}\right]^{\frac{1}{3}} \quad \text{and} \quad b = \frac{1}{6} \left[\frac{1}{\tau_0^2 \Delta\Theta_{of}}\right]^{\frac{1}{3}}. \quad (60)$$

Therefore, linear regression methods can be used to obtain estimators of a and b , which, from a statistical point of view are random variables, [3], [8]. From estimators of a and b , $\Delta\Theta_{of}$ and τ_0 estimators can be derived as follows:

$$\Delta \hat{\Theta}_{of} = \frac{1}{6\hat{a}^2\hat{b}} \quad \text{and} \quad \hat{\tau}_0 = \frac{\hat{a}}{6\hat{b}}. \quad (61)$$

This methodology allows the determination of parameters variability from an estimator variability; according to recent usual recommendations, [23], the variation coefficients of the parameters, denoted by $CV_{\Delta\theta_f}$ and CV_{τ} , can be approximately evaluated by uncertainty propagation of corresponding variances:

$$CV_{\Delta\theta_f} \approx \sqrt{4(CV_a)^2 + (CV_b)^2} \quad \text{and} \quad (62)$$

$$CV_{\tau_0} \approx \sqrt{(CV_a)^2 + (CV_b)^2}$$

Concerning the test duration, this methodology reduces the test duration required by [11] because relatively accurate values for the parameters can be estimated only from the beginning of the exponential trajectory, with $t < 2\tau_0$. This alternative methodology will be referred as *Limited Period Methodology* (LPM).

From the basics of linear regression, a minimum of two data values ($N=2$) is required to estimate parameter values. However, and with the usual assumption that residuals are normally distributed, its second moment (variation) estimation do involves the calculus of a t -Student distribution with $N-2$ degrees of freedom. Therefore, although $N=2$ allows the parameters estimation, the corresponding variability determination requires $N \geq 3$ [3], [20].

Moreover the initial pair of measurements ($t=0$; $\Delta\Theta_{o0}=0$) can not be part of the measurements set; the function to which linear regression is applied is, itself, a function of the ratio $t/\Delta\Theta_o$ and thus, initial pair of measurements would lead to a mathematical in determination.

B3. Simulated Case Studies

In order to evaluate the accuracy of the concurrent methodologies, the data set of the heat run test was simulated. With such a procedure, correct values of parameters $\Delta\Theta_{of}$ and τ_0 are known in advance and therefore, errors of estimators given by the two methodologies can be evaluated. Following the first order model of International Standards, data for the simulated heat run test was assumed to follow a deterministic single exponential function, representing transformer thermal behaviour from no-load to rated load. To represent the uncertainties of the measuring process an additive perturbation such as random gaussian white noise with a null mean and variance σ^2 , generated with a Monte Carlo method [22], [17], was considered:

$$\Delta\Theta_0(t) = \Delta\Theta_{of} \left(1 - e^{-\frac{t}{\tau_0}} \right) + N(0, \sigma). \quad (63)$$

For a distribution transformer rated 630 kVA, 10 kV/400 V, considered values for parameters are: $\Delta\Theta_{of}=55$ K and

$\tau_0=2$ h. Test data was generated up to $t_{max}=12$ h and with a time step $\Delta t_{meas}=0.25$ h.

Four data sets were generated considering realistic σ values and Table 6 specifications. Sample lengths are $N=100$ thus Monte Carlo inherent errors are lower than σ .

Table 6. Case studies specifications.

| Specificati on | σ [K] | Equidistant measurements | Truncation | t_{max}/τ_0 |
|----------------|--------------|--------------------------|------------|------------------|
| Set n°1 | 0.5 | Equidistant. | 0- 12 h | 6 |
| Set n°2 | 1 | Equidistant | 0- 8 h | 4 |
| Set n°3 | 1 | Non-Equidistant | 0- 3 h | 1,5 |
| Set n°4 | 1 | Non-Equidistant | 1- 4 h | 2 |

Simulated data referred as Set n°3 and set n°4 are represented on Figure 14. Both time scale t and reduced time scale t/τ_0 are represented. Set n°1 specifications are almost ideals since it is the most favourable for Standards methodology; white noise is of reduced variation and measurements are performed at equidistant intervals. Set n°2 is more realistic; it is similar to n°1 but with a doubling white noise variation. Set n°3 presents the same level of white noise as set n°2 but measurements are not equidistant and data series was truncated on its high limit, drastically reducing test duration.

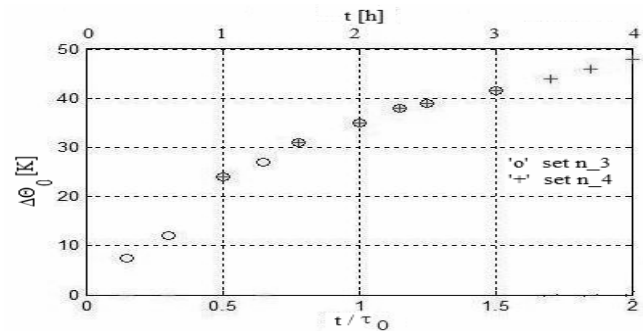


Fig. 14 - Heat-run test data, set n°3 and set n°4.

Set n°4 is similar to set n°3 except for truncation limits; data set window was shifted one hour later.

B4. Results for International Standards Methodologies

These results are resumed on Table 7. Set n° 1 is the only one fulfilling [11] criterion to end the test at 11 hours ($\approx 5.5\tau_0$). The TPM did not converge (n.c) for τ_0 estimation on set n°1, Figure 15, nevertheless, conditions stated by [11] are fulfilled since time interval Δt between Θ_{o1} , Θ_{o2} and Θ_{o3} is of the same magnitude as τ_0 and represented values fulfil the condition $\Delta\Theta_{o3}/\Delta\Theta_{of} < 0.95$. It did not converge either for $\Delta\Theta_{of}$ or τ_0 on set n°2. This methodology can not be applied on sets n°3 and 4, since data measurements are not equidistant. LSM provide admissible results for all tests; however its accuracy is reduced for set n°4, to which corresponds a very short test duration.

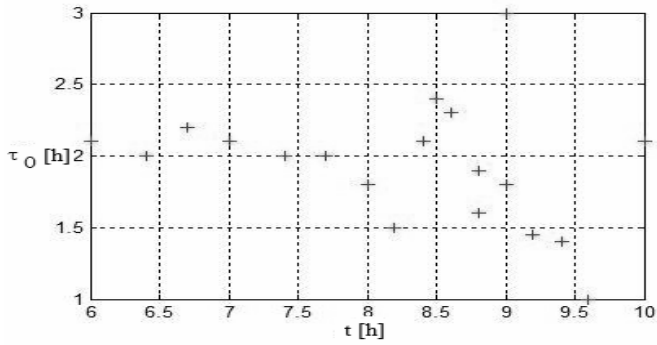


Fig. 15 - Estimated τ with (54) and data set n°1 (TPM).

Table 7. International Standards methodology results (TPM and LSM).

| | Set n°1 | | Set n°2 | | Set n°3 | | Set n°4 | |
|-----|---------------------|----------|---------------------|----------|---------------------|----------|---------------------|----------|
| | $\Delta\Theta_{of}$ | τ_0 | $\Delta\Theta_{of}$ | τ_0 | $\Delta\Theta_{of}$ | τ_0 | $\Delta\Theta_{of}$ | τ_0 |
| TPM | 55.0 | n.c. | n.c. | n.c. | - | - | - | - |
| LSM | 55.3 | 2.03 | 56.0 | 2.15 | 48.5 | 1.53 | 50.3 | 1.63 |

B5. Results for Alternative Methodology

Since the systematic error (57) of LPM is dependent upon the ratio t/τ_0 , most relevant results of each of the four considered sets are represented in a graphical form; Figure 16 to Figure 19 represent successive estimates of parameters, as a function of increasing cumulative data from tests.

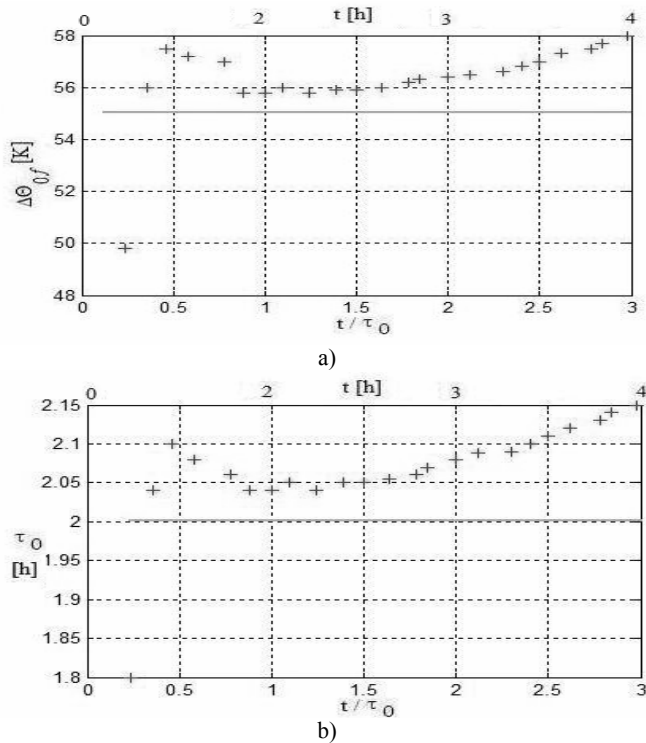


Fig. 16 - Mean value of $\Delta\Theta_f$ (a) and τ (b) estimated with LPM. (data set n°1).

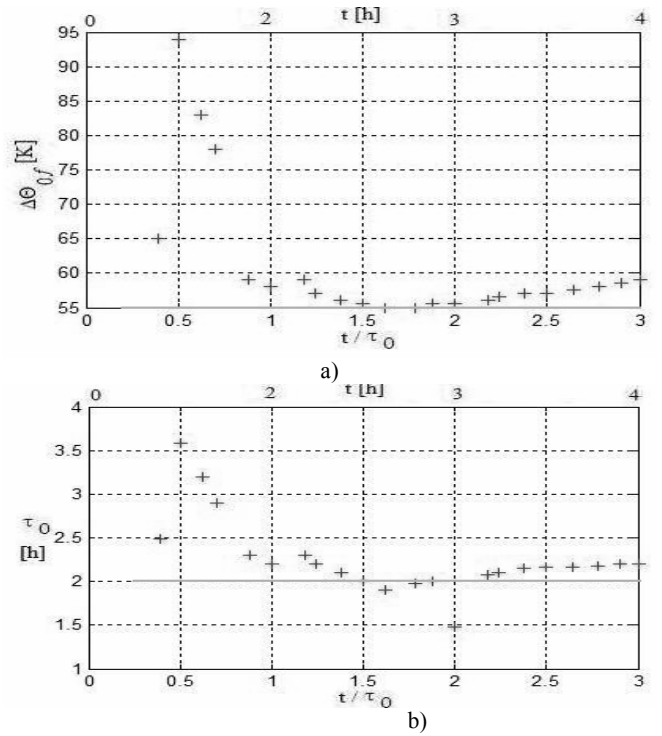


Fig. 17 - Mean value of $\Delta\Theta_f$ (a) and τ (b) estimated with LPM. (data set n°2).

Exact values of the parameters to be estimated are also represented as dotted lines.

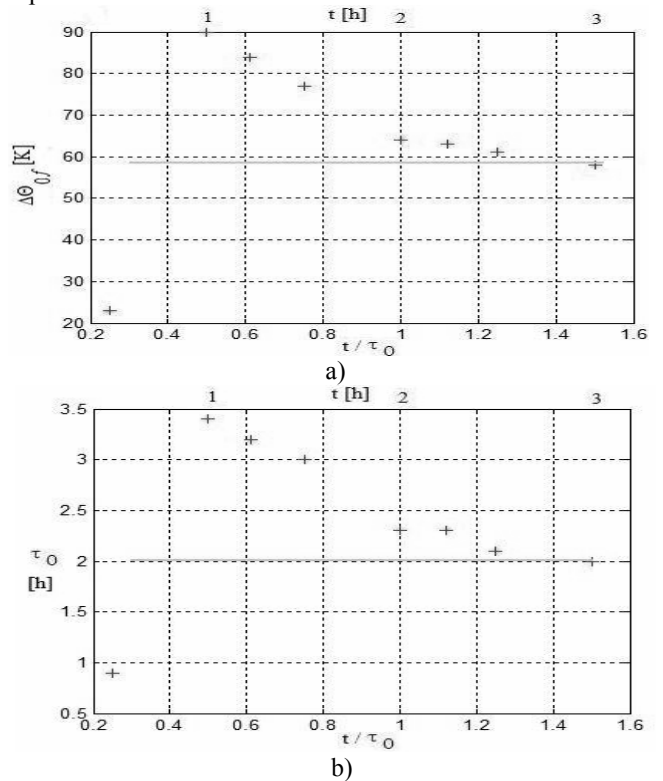


Fig. 18 - Mean value of $\Delta\Theta_f$ (a) and τ (b) estimated with LPM. (data set n°3).

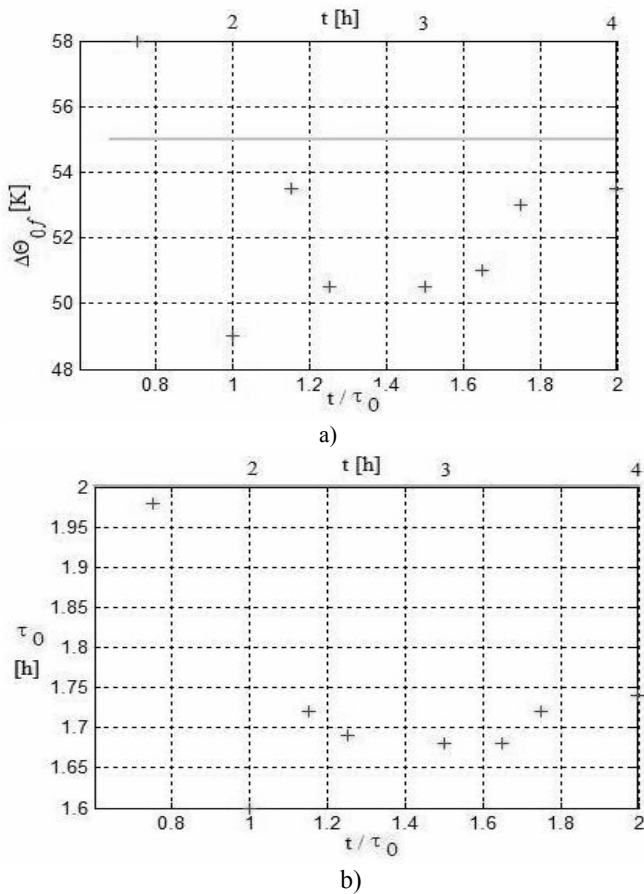


Fig. 19 - Mean value of $\Delta\Theta_f$ (a) and τ (b) estimated with LPM. (data set n°4).

B6. LPM Previous Considerations and Efficiency Criterion

The approximation of the increasing exponential function (53) by a polynomial function, (41), gives rise to a systematic error of LPM, which is given by (57). This error and its majoring (43) are represented in Figure 20 as a function of the ratio t/τ_0 . In order to reduce this error, data to apply LPM must belong to the lower part of the heating curve (reduced t/τ_0 values). This error explains the increasing time drift of estimated parameter values for high t/τ_0 values, most visible on Figure 16.

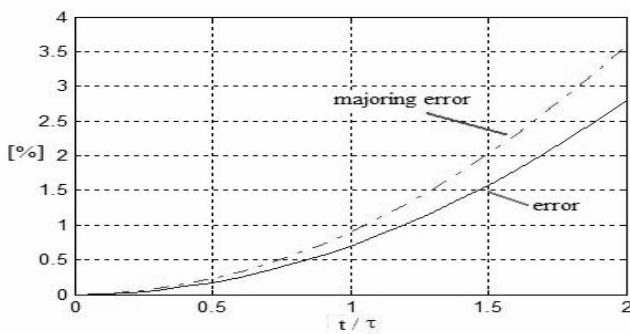


Fig. 20 - LPM systematic error, ϵ_S and its majoring, ϵ_M .

This mathematical constrain is traduced by an economical advantage since the duration of the required transformer heat-run tests is substantially reduced relatively to International Standards requirements. From the linear regression theory, however, to parameters estimated with a reduced number of data measurements, a high variability coefficient is associated [3]. The first estimated parameters represented on Figure 16 to Figure 19 ($0 < t/\tau_0 < 1$) do present a high error; however, to these values great variability coefficients are associated which, traduced by the corresponding 95% confidence interval, will include the exact $\Delta\Theta_{of}$ and τ_0 values. It is not the purpose of any methodology to estimate parameters with such a high variability, corresponding to unrealistic situations. Therefore, a compromise must be achieved between a sufficient number of data measurements but within a t/τ_0 interval constrained by the systematic error represented on Figure 20. This work proposes that approximately 10 measurements ($N=10$), in a range below $1.5 t/\tau_0$, must be considered. Comparison of results obtained with data sets n°3 and n°4 will exemplify the importance of this upper limit. While set n°3, by respecting this observation constraint (upper limit is $1.5t/\tau_0$), gives very good results, set n°4, with a similar observation window length but shifted one hour (upper limit is $2t/\tau_0$), evidences a degradation of results.

Taking into account previous considerations and results (Figure 16 to Figure 19) it is possible to propose a simple criterion for obtaining an accurate set of $(\Delta\Theta_{of}, \tau_0)$ estimators. After Figure 16 to Figure 19, one realises that best $(\Delta\Theta_{of}, \tau_0)$ estimators are obtained within the range τ_0 to $2\tau_0$ and thus on the vicinity of $1.5\tau_0$. A-priori, τ_0 is unknown, and thus, so are τ_0 and ϵ_M . Therefore, estimates of these values (denoted by $t/\hat{\tau}_0$ and $\hat{\epsilon}_M$) should be determined, at each instant, using the correspondent τ_0 estimation (denoted by $\hat{\tau}_0$). On Table 8 to Table 11, information concerning observed data (t and N), $\Delta\Theta_{of}$ and τ_0 estimators (mean and variation coefficients) and t/τ_0 and ϵ_M estimators, is regrouped.

Table 8. LPM results for Set n°1.

| Data | | $\Delta\hat{\Theta}_{of}$ | | $\hat{\tau}_0$ | | LPM | |
|-------------|-----------|---------------------------|-------------|----------------|-------------|----------------------|------------------------|
| t [h] | N | μ [° C] | CV[%] | μ [h] | CV[%] | $t/\hat{\tau}_0$ [%] | $\hat{\epsilon}_M$ [%] |
| 2.00 | 8 | 55.65 | 1.31 | 2.02 | 1.29 | 0.99 | 0.45 |
| 2.25 | 9 | 55.85 | 1.05 | 2.03 | 1.03 | 1.11 | 0.63 |
| 2.50 | 10 | 55.77 | 0.85 | 2.03 | 0.83 | 1.23 | 0.86 |
| 2.75 | 11 | 55.83 | 0.70 | 2.03 | 0.68 | 1.35 | 1.15 |
| 3.00 | 12 | 55.85 | 0.59 | 2.03 | 0.57 | 1.48 | 1.49 |

Table 9. LPM results for Set n°2.

| Data | | $\Delta\hat{\Theta}_{of}$ | | $\hat{\tau}_0$ | | LPM | |
|-------------|-----------|---------------------------|-------------|-----------------|-------------|----------------------|------------------------|
| t[h] | N | $\mu[^\circ\text{C}]$ | CV[%] | $\mu[\text{h}]$ | CV[%] | $t/\hat{\tau}_0$ [%] | $\hat{\epsilon}_M$ [%] |
| 2.00 | 8 | 56.97 | 14.09 | 2.07 | 13.87 | 0.97 | 0.42 |
| 2.25 | 9 | 58.11 | 11.29 | 2.11 | 11.09 | 1.07 | 0.56 |
| 2.50 | 10 | 56.19 | 9.01 | 2.03 | 8.80 | 1.25 | 0.88 |
| 2.75 | 11 | 55.63 | 7.35 | 2.00 | 7.15 | 1.38 | 1.20 |
| 3.00 | 12 | 54.75 | 6.18 | 1.97 | 5.97 | 1.55 | 1.69 |

Table 10. LPM results for Set n°3.

| Data | | $\Delta\hat{\Theta}_{of}$ | | $\hat{\tau}_0$ | | LPM | |
|-------------|----------|---------------------------|-------------|-----------------|-------------|----------------------|------------------------|
| t[h] | N | $\mu[^\circ\text{C}]$ | CV[%] | $\mu[\text{h}]$ | CV[%] | $t/\hat{\tau}_0$ [%] | $\hat{\epsilon}_M$ [%] |
| 2.00 | 6 | 62.89 | 16.63 | 2.32 | 16.44 | 0.86 | 0.30 |
| 2.25 | 7 | 61.49 | 11.78 | 2.26 | 11.59 | 1.00 | 0.46 |
| 2.50 | 8 | 57.79 | 9.60 | 2.09 | 9.38 | 1.20 | 0.79 |
| 3.00 | 9 | 55.56 | 7.51 | 1.99 | 7.26 | 1.51 | 1.59 |

Table 11. LPM results for Set n°4.

| Data | | $\Delta\hat{\Theta}_{of}$ | | $\hat{\tau}_0$ | | LPM | |
|-------------|----------|---------------------------|-------------|----------------|----------|-----------------------|-------------|
| t[h] | N | $\mu[^\circ\text{C}]$ | CV[%] | t[h] | N | $\mu[^\circ\text{C}]$ | CV[%] |
| 3.00 | 3 | 49.12 | 10.38 | 3.00 | 3 | 49.12 | 10.38 |
| 3.25 | 4 | 52.15 | 3.90 | 3.25 | 4 | 52.15 | 3.90 |
| 3.50 | 5 | 50.45 | 3.00 | 3.50 | 5 | 50.45 | 3.00 |
| 4.00 | 6 | 50.49 | 1.99 | 4.00 | 6 | 50.49 | 1.99 |

Due to the non-linear transformation used by LPM (59), statistical errors, CV, simultaneously depend upon N and σ (measurements variability) which, *a-priori*, are unknown parameters. A quantitative quality criterion is of difficult establishment due to errors dependence upon unknown parameters such as σ and τ_0 . Therefore, an heuristic qualitative criterion is proposed, as following: to consider approximately 10 successive measurements and determine respective $\Delta\hat{\Theta}_{of}$ and $\hat{\tau}_0$ values, within a range $0 < t/\hat{\tau}_0 < 1.5$. A reasonably accurate set of $(\Delta\Theta_{of}, \tau_0)$ estimators is obtained for $t/\hat{\tau}_0 \sim 1.5$. If $t/\hat{\tau}_0$ range can not be fulfilled (which is the case of set n°4), estimators corresponding to the lowest $t/\hat{\tau}_0$ values, should be considered. Application of this qualitative criterion leads to the conclusion that best bidimensional estimators $(\Delta\Theta_{of}, \tau_0)$ are obtained for N=12 (on set n°1), N=12 (on set n°2), N=9 (on set n°3) and N=4 (on set n°4). These values are represented on bold face font on Table 8 to Table 11.

B7. Comparative Analysis

Table 12 regroups International Standards (Table 7 for TPM and LSM) and LPM (Table 8 to Table 11) methodologies results giving the estimated parameter errors,

as percentage values of correct ones $\Delta\Theta_{of}=55\text{ K}$ and $\tau_0=2\text{ h}$.

The duration of the test to achieve corresponding results is also represented (t_{max}). For LPM, values after the section §5.B6 criterion are represented.

Table 12. Parameter errors [%] for concurrent methodologies.

| | Set n°1 | | Set n°2 | | Set n°3 | | Set n°4 | |
|--|---------------------|----------|---------------------|----------|---------------------|----------|---------------------|----------|
| | $\Delta\Theta_{of}$ | τ_0 | $\Delta\Theta_{of}$ | τ_0 | $\Delta\Theta_{of}$ | τ_0 | $\Delta\Theta_{of}$ | τ_0 |
| International Standards Methodology | | | | | | | | |
| t_{max} | 11 h | | 8h | | 3h | | 4h | |
| TPM | 0.0 | n.c. | n.c. | n.c. | | | | |
| LSM | 0.19 | 0.51 | 1.81 | 7.00 | -11.81 | -24.00 | 8.73 | -18.7 |
| Alternative Methodology LPM for $1 < t/\hat{\tau}_0 < 1.5$ | | | | | | | | |
| t_{max} | 3h | | 3h | | 3h | | 3.25 h | |
| | 1.55 | 1.51 | -0.49 | -2.51 | 1.03 | -0.51 | 5.19 | -14.4 |

International Standards methodologies (TPM and LSM) give very good estimations for set n°1 but they require 11 hours of run test, while LPM methodology provides sufficiently accurate values after 3 hour of testing. For set n°2, LPM provides better estimators and after, approximately, less than 1/2 of the test duration required by International Standards (TPM and LSM). For set n°3, estimations given by LPM are clearly better than those provided by International Standards (LSM) for the same test duration. Although data of set n°4 does not fulfil LPM requirements, it provides better estimators than LSM and with reducer test duration.

VI. CONCLUSION

In order to study transformers thermal loss of life, complex models taking into account electrical and thermal characteristics are required. Moreover, the precision of thermal models is dependent upon the exactitude of the parameters. The work presented in this article shows that, through electromagnetic similitude laws, one can obtain, for an homogeneous series of transformers with different rated powers, the main parameters required for the thermal model. The foremost advantage of this methodology is its compactness, since parameters are obtained only from the knowledge of transformer rated power. Theoretical results were compared with data from transformer manufacturers and the good agreement between both validates theoretical results.

Due to data variation one can not conclude whether, within the considered power range, the rated current density should be considered constant or not; due to data variation, results from both hypotheses are satisfactory.

As will be studied on future, the exactitude of thermal parameters "thermal time constant" and, mainly, "final temperature rise", is determinant on thermal model accuracy.

Usually, these parameters are obtained from standardised heat-run tests and their correct measurement is of difficult precision due to data measurement variability. In this article, an easy and efficient method to estimate these thermal parameters, as well as the corresponding using criteria, were proposed. This robust methodology presents advantages relatively to the standardised methodologies, since it allows a considerably reduction on test duration, and provides results which are always physically acceptable and with measurable precision.

REFERENCES

- [1] I. Borcosi, Onisifor O., M.C. Popescu, A. Dincă, "A Method to Protect from no Pulse for a Three-Phase Rectifier Bridge Connected with the Resistive-Inductive Load", *Proceedings of the 10th WSEAS International Conference on Mathematical and Computational Methods in Science and Engineering (MACMESE'08)*, pp.146-152, Bucharest, Romania, November 7-9, 2008.
- [2] C.A. Bulucea, M.C. Popescu, C.A. Bulucea, Gh. Manolea, A. Patrascu, "Interest and Difficulty in Continuous Analysis of Water Quality", *Proceedings of the 4th IASME/WSEAS International Conference on Energy & Environment (EE'09)*, Cambridge, pp.220-225, Feb.22-23, 2009.
- [3] Bulucea C.A., M.C. Popescu, Bulucea C.A., Patrascu A., Manolea Gh., "Real Time Medical Telemonitoring of Sustainable Health Care Measuring Devices", *Proceedings of the 8th WSEAS Int. Conf. on Artificial Intelligence, Knowledge Engineering & Data Bases (AIKED '09)*, Cambridge, pp.202-207, Feb.22-23, 2009.
- [4] S.A. Efacec, *Distribution Transformers Data Sheet*, 1993.
- [5] Z. Godec, "New Method for determination of steady-state temperature rises of transformers", *IEEE Proceedings*, Vol. 131, Pt. A. n°5, pp. 307-311, 1984.
- [6] Z. Godec, "Determination of steady-state temperature rises of power transformers", *IEEE Proceedings*, Vol. 134, Pt. A. n°10, pp.773-778. 1987.
- [7] A. Granino, "Mathematical Handbook for Scientists and Engineers", McGraw-Hill, 1968.
- [8] L. Gutmann, S. Wilks, J.S. Hunter, "Introductory Engineering Statistics", 3rd Edition, John Wiley&Sons, 1982.
- [9] IEEE, "PES Transformers Committee, Background Information on High Temperature Insulation for Liquid-Immersed Power Transformers", *IEEE Transaction on Power Delivery*, Vol. 9, n°4, pp.1892-1906, 1994.
- [10] IEC-76, Part 1, "International Electrotechnical Commission, Power Transformers Temperature Rise", Second Edition, 1993.
- [11] IEC-76, Part 2, "International Electrotechnical Commission, Power Transformers Temperature Rise", Second Edition, 1993.
- [12] IEC-354, "International Electrotechnical Commission, Loading Guide for Oil-Immersed Power Transformers", Second Edition, 1991.
- [13] N. Mastorakis, C.A. Bulucea, M.C. Popescu, Gh. Manolea, L. Perescu, "Electromagnetic and Thermal Model Parameters of Oil-Filled Transformers", *WSEAS Transactions on Circuits and Systems*, Issue 6, Volume 8, pp.475-486, June 2009.
- [14] N. Mastorakis, C.A. Bulucea, M.C. Popescu, "Transformer Electromagnetic and Thermal Models", *9th WSEAS International Conference on Power Systems (PS'09): Advances in Power Systems*, pp.108-117, Budapest, Hungary, September 3-5, 2009.
- [15] N. Mastorakis, C.A. Bulucea, Gh. Manolea, M.C. Popescu, L. Perescu-Popescu, "Model for Predictive Control of Temperature in Oil-filled Transformers", *Proceedings of the 11th WSEAS International Conference on Automatic Control, Modelling and Simulation*, pp.157-165, Istanbul, Turkey, may 30-1 June 2009.
- [16] L. Pierrat, "Méthode d'Identification et Analyse d'Incertitude pour les Paramètres d'une Courbe d'Echauffement Tronquée", *8th International Congress of Metrology*, Besacon, 1997.
- [17] M.C. Popescu, C.A. Bulucea, Manolea Gh., L. Perescu, "Parameters Modelling of Transformer", *WSEAS Transactions on Circuits and Systems*, Issue 8, Volume 8, August 2009.
- [18] M.C. Popescu, "Three Connectionist Implementations of Dynamic Programming for Optimal Control", *Journal of Advanced Research in Fuzzy and Uncertain Systems*, Vol.1, No.1, pp.1-16, Mar. 2009.
- [19] M.C. Popescu M.C., V.E. Balas, Gh. Manolea, L. Perescu, N. Mastorakis, "Theoretical and Practical Aspects of Heating Equation", *WSEAS Transactions on Systems and Control*, Issue 8, Volume 4, August 2009.
- [20] M.C. Popescu M.C., V.E. Balas, L. Perescu-Popescu, N. Mastorakis, "Multilayer Perceptron and Neural Networks", *WSEAS Transactions on Circuits and Systems*, Issue 7, Volume 8, pp.579-588, July 2009.
- [21] M.C. Popescu, N. Mastorakis, C.A. Bulucea, Gh. Manolea L. Perescu, "Non-Linear Thermal Model for Transformers Study", *WSEAS Transactions on Circuits and Systems*, Issue 6, Volume 8, pp.487-497, June 2009.
- [22] M.C. Popescu, M.C., Gh. Manolea, C.A. Bulucea, L. Perescu-Popescu, Drighiciu M.A., "Modelling of Ambient Temperature Profiles in Transformer", *Proceedings of the 13th WSEAS International Conference on Circuits*, (part of the 13th WSEAS CSCC Multiconference) pp.128-137, Rodos, Greece, July 22-24, 2009..
- [23] M.C. Popescu, Gh. Manolea, C.A. Bulucea, N. Boteanu, L. Perescu-Popescu, I.O. Muntean, "Transformer Model Extension for Variation of Additional Losses with Frequency", *Proceedings of the 11th WSEAS International Conference on Automatic Control, Modelling and Simulation*, pp.166-171, Istanbul, Turkey, may 30-1 June 2009.
- [24] M.C. Popescu, V.E. Balas, Gh. Manolea, N. Mastorakis, "Regional Null Controllability for Degenerate Heat Equations", *Proceedings of the 11th WSEAS International Conference on Sustainability in Science Engineering*, pp.32-37, Timisoara, Romania, may 27-29, 2009.
- [25] M.C. Popescu, V.E. Balas, L. Popescu, "Heating Monitored and Optimal Control of Electric Drives", *3rd International Workshop on Soft Computing Applications*, Proceedings IEEE Catalog Number CFP0928D-PRT, Library of Congress 2009907136, pp.149-155, Szeged-Hungary-Arad-Romania, 26 July-1 August, 2009
- [26] M.C. Popescu, M.M. Balas, "Thermal Consumptions : Control and Monitoring". *3rd International Workshop on Soft Computing Applications*, Proceedings IEEE Catalog Number CFP0928D-PRT, Library of Congress 2009907136, pp.85-91, Szeged-Hungary-Arad-Romania, 26 July-1 August 2009.